

Supporting Information

Improving the flame retardant property of bottle grade PET foam made by reactive foam extrusion

*Christian Bethke, Tobias Standau, Daniela Goedderz, Lais Weber, Manfred Döring², Volker Altstädt**

Supporting to 3.1 Foam extrusion and 3.2 Foam properties

With the optimized parameters and mixtures listed in **Table 1**, a stable and reproducible processing of the PET foams without calibration was possible. However, due to the required calibration step, the resulting foam morphology and density got difficult to control. The processing parameters, density values and DSC results of the 2nd heating curve are summarized in **Table S1**.

Table s1. Overview of PET-Foam samples, its chain extender (PMDA) and flame retardant (FR) content by wt. %. Additionally, the extrusion temperature at die (T_D) and melt (T_M) and resulting foam properties of the results DSC 2nd heating ramp regarding glass transition temperature (T_g), melting temperature (T_m) and crystallinity (ΔH and X) are presented.

Sample	PMDA [wt %]	FR [wt %]	T_D [°C]	T_M [°C]	T_g [°C]	T_m [°C]	Cryst. ΔH [J g ⁻¹]	Cryst.X [%]
unfoamed PET	-	-	-	-	81	249	32	22,86
CE-PET V1	0.25	0	255	254	81	242	30	21,43
CE-PET V2	0.33	0	245	250	80	242	31	22,14
5 % DEPZn	0.35	5	255	250	82	242	27	19,29
5 % HFR	0.25	5	250	255	82	240	30	21,43
3% PSMP	0.35	3	255	250	81	240	30	21,43
2% PSMP ^{a)}	0.4	2	240	247	79	243	34	24,29
2 % DOP	0.35	2	245	248	80	243	31	22,14
Commercial	-	-	-	-	75	237	32	22,86

a) contains ZnSt in a 20:1 ratio PSMP:ZnSt

Due to the calibration process after foam extrusion a piling of the foam takes place which enables the formation of air pockets which are larger than the foam cells. This effect is schematically shown in **Figure S1**.

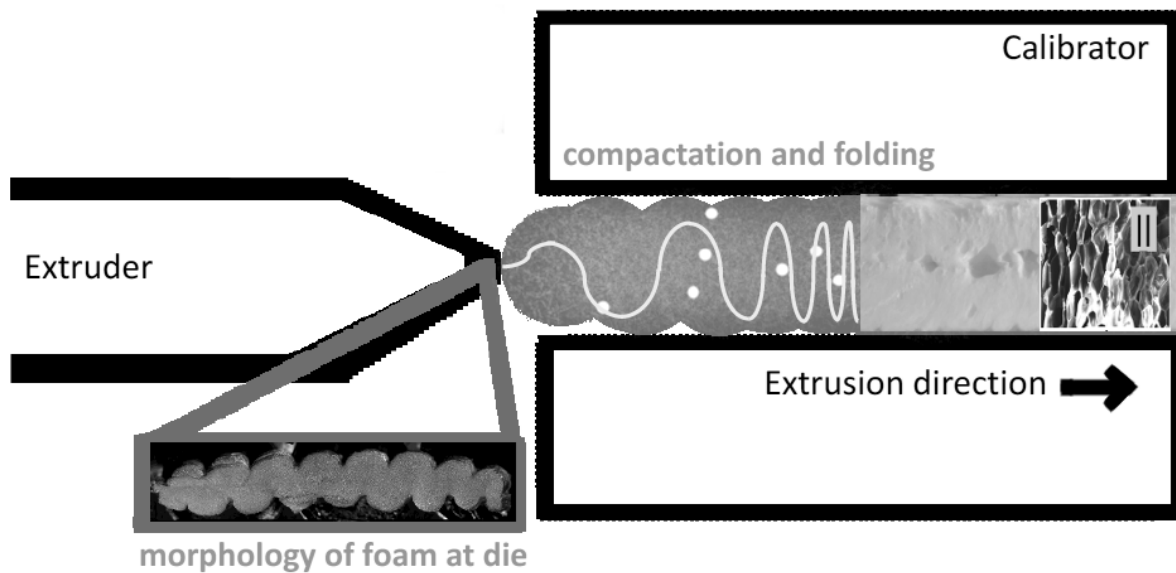


Figure S1. Entrapping of air and piling effect during calibration. The wave like structure received from the slit die is additionally folded and stacked.

Supporting to 3.3 Fire Behavior

The heat release over time and total heat release development of the foamed samples are shown in the supporting information **Figure S2a**, while the development of smoke release is shown in **Figure S2b**.

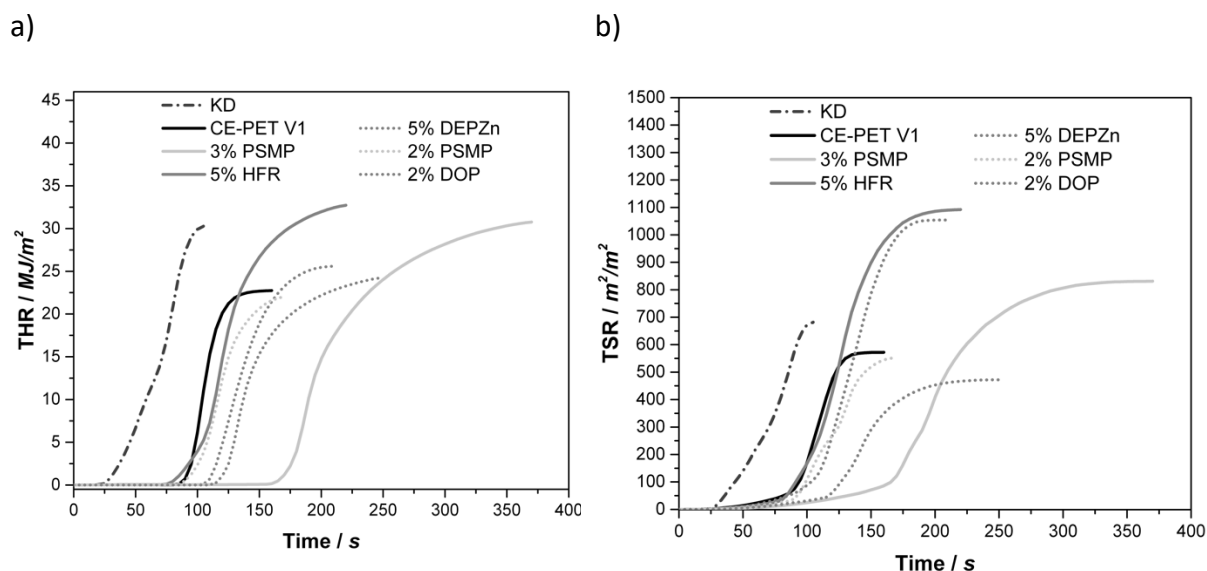


Figure S2. a) Development of THR and b) of TSR during the measurement of the different samples investigated at 35 kW m⁻² heatflux and 25mm gap.

The detail results of the single-flame source tests are presented in **Table S2**.

TABLE s2. Results of the single-flame source test according to EN ISO 11935-2 of the different PET foams.

sample	Foam density [g l ⁻¹]	Average flame spread [s]	EN ISO 11935-2 classification	dripping	Burning dripping
CE-PET V1	157 ± 8	1.22	E	yes	no
PET V2	253 ± 9	0.8	E	yes	no
5 wt % DEPZn	215 ± 34	0.2	E	yes	no
5 wt% HFR	253 ± 24	1.3	E	yes	no
3 wt% PSMP	401 ± 78	0	E	yes	no
2 wt% PSMP ^{a)}	221 ± 16	0	E	yes	no
2 wt% DOP	245 ± 16	0	E	yes	no
KD	190 ± 15	8.6	E d2	Yes	yes

a) contains ZnSt in a 20:1 ratio PSMP:ZnSt

Supporting to 3.4 Mechanical testing

Table S3 summarizes the uncorrected results of the compression testing results of

$10 \times 10 \times 10 \text{ mm}^3$ cubes, tested with 1 mm/min speed.

Table S3. Numerical results of the compressive tests nominal and corrected by density. The compression values for E-Modulus (E_{Cs}) and stress at 10% strain ($\sigma_{Cs10\%}$) were determined for horizontal (h) and vertical (v) orientation.

Sample		E_{Cs} nom [MPa]	E_{Cs} cor. [MPa]	$\sigma_{Cs10\%}$ nom. [MPa]	$\sigma_{Cs10\%}$ cor. [MPa]
CE-PET V1	0	1.09 ± 0.49	0.0069 ± 0.0031	0.08 ± 0.02	0.0004 ± 0.0002
	90	3.41 ± 1.46	0.0217 ± 0.0093	0.74 ± 0.31	0.0047 ± 0.0020
5 wt% DEPZn	0	5.10 ± 1.23	0.0264 ± 0.0064	0.51 ± 0.28	0.0027 ± 0.0014
	90	6.84 ± 2.04	0.0354 ± 0.0106	1.14 ± 0.48	0.0059 ± 0.0025
5 wt% HFR	0	2.32 ± 1.02	0.0092 ± 0.0041	0.28 ± 0.02	0.0011 ± 0.0004
	90	92.70 ± 22.09	0.3664 ± 0.0873	3.26 ± 0.26	0.0129 ± 0.0010
3 wt% PSMP	0	16.54 ± 6.25	0.0749 ± 0.0283	0.98 ± 0.25	0.0044 ± 0.0011
	90	36.83 ± 25.27	0.1666 ± 0.1164	1.56 ± 0	0.0070 ± 0
2 wt% PSMP ^{a)}	0	14.03 ± 8.27	0.0350 ± 0.0206	1.25 ± 0.38	0.0031 ± 0.0010
	90	15.22 ± 8.94	0.0380 ± 0.0223	3.47 ± 0.44	0.0074 ± 0.0020
2 wt% DOP	0	39.36 ± 17.16	0.1606 ± 0.0700	2.83 ± 0.27	0.0116 ± 0.0011
	90	48.22 ± 14.40	0.1968 ± 0.0588	4.5 ± 1.24	0.0184 ± 0.0051
KD	0	43.19 ± 9.32	0.2274 ± 0.0491	2.04 ± 0.31	0.0108 ± 0.0017
	90	54.26 ± 11.75	0.2856 ± 0.0619	2.73 ± 0.38	0.0144 ± 0.0020

a) contains ZnSt in a 20:1 ratio PSMP:ZnSt

Table S4 summarizes the uncorrected values of the three-point bending tests of

$60 \times 25 \times 10 \text{ mm}^3$ samples, tested with 10mm/min speed and an effective span of 50mm.

Table S4. Numerical results of the three-point bending tests. nominal (nom.) and corrected by density (cor.). The bending E-Modulus (E_{Bs}) and stress at break ($\sigma_{Bs10\%}$) were evaluated in vertical (90°) direction only.

Sample	E_{Bs} nom. [MPa]	E_{Bs} cor. [MPa]	σ_{Bs} nom. [MPa]	σ_{Bs} cor. [MPa]
CE-PET V1	2.07 ± 0.28	0.01 ± 0	0.26 ± 0.04	0.14 ± 0.02
5 wt% DEPZn	24.18 ± 10.46	0.13 ± 0.05	4.26 ± 0.37	2.21 ± 0.19
5 wt% HFR	31.63 ± 8.29	0.33 ± 0.09	8.90 ± 0.64	9.35 ± 0.67
3 wt% PSMP	27.89 ± 16.38	0.13 ± 0.07	8.66 ± 0.47	3.92 ± 0.21
2 wt% PSMP ^{a)}	74.20 ± 15.81	0.19 ± 0.04	14.04 ± 1.93	0.19 ± 0.04
2 wt% DOP	17.99 ± 7.40	0.07 ± 0.03	1.65 ± 0.82	0.67 ± 0.34
KD	52.178 ± 12.83	0.27 ± 0.07	3.01 ± 0.42	1.58 ± 0.22

a) contains ZnSt in a 20:1 ratio PSMP:ZnSt